

# Design of non-periodic dielectric stacks for tailoring the emission of organic lighting-emitting diodes

Mukul Agrawal and Peter Peumans\*

Electrical Engineering Department, Stanford University, Stanford, CA 94305

\*Corresponding author: [ppeumans@stanford.edu](mailto:ppeumans@stanford.edu)

<http://www.stanford.edu/~ppeumans>

**Abstract:** The majority of photons emitted in organic light-emitting diodes are either trapped in the substrate or emitted into lossy waveguided modes. We show how optimized, non-periodic dielectric stacks inserted between the substrate and transparent anode can be used to improve the photon outcoupling efficiency by tailoring of the local photon density of states. Unlike previously demonstrated outcoupling schemes, this method does not lead to pixel blurring and maintains a Lambertian angular emission profiles within a specified cone. For small molecular weight, green-emitting devices, a 2.5-fold uniformly distributed increase in brightness is achievable for a viewing angle of 60°.

©2007 Optical Society of America

OCIS codes: (230.3670) Light-emitting diodes; (310.1620) Coatings.

---

## References and links

1. P. A. Hobson, S. Wedge, J. A. E. Wasey, I. Sage and W. L. Barnes, "Surface plasmon mediated emission from organic light-emitting diodes," *Adv. Mater.* **14**, 1393-1396 (2002).
2. P. T. Worthing and W. L. Barnes, "Efficient coupling of surface plasmon polaritons to radiation using a bi-grating," *Appl. Phys. Lett.* **79**, 3035-3037 (2001).
3. C. F. Madigan, M. H. Lu and J. C. Sturm, "Improvement of output coupling efficiency of organic light-emitting diodes by backside substrate modification," *Appl. Phys. Lett.* **76**, 1650-1652 (2000).
4. S. Møller and S. R. Forrest, "Improved light out-coupling in organic light emitting diodes employing ordered microlens arrays," *J. Appl. Phys.* **91**, 3324-3327 (2002).
5. T. Tsutsui, M. Yashiro, H. Yokogawa, K. Kawano, M. Yokoyama, "Doubling coupling-out efficiency in organic light-emitting devices using a thin silica aerogel layer," *Adv. Mater.*, **13**, 1149-1152 (2001)
6. L. H. Smith, J. A. Wasey, W. L. Barnes, "Light outcoupling efficiency of top-emitting organic light-emitting diodes," *Appl. Phys. Lett.* **84**, 2986-2988 (2004).
7. T. Nakayama, Y. Itoh and A. Kakuta, "Organic photo- and electroluminescent devices with double mirrors," *Appl. Phys. Lett.* **63**, 594-595 (1993).
8. T. Tsutsui, N. Takada and Shogo Saito, "Sharply directed emission in organic electroluminescent diodes with an optical-microcavity structure," *Appl. Phys. Lett.* **65**, 1868-1870 (1994).
9. S. Fan, P. R. Villeneuve and J. D. Joannopoulos, "High extraction efficiency of spontaneous emission from slabs of photonic crystals," *Phys. Rev. Lett.* **78**, 3294-3297 (1997)
10. J. Vuckovic, M. Loncar and A. Scherer, "Surface plasmon enhanced light-emitting diodes," *IEEE J. Quantum Electron.* **36**, 1131-1144 (2000).
11. A. Dodabalapur, L. J. Rothberg, R. H. Jordan, T. M. Miller, R. E. Slusher, and Julia M. Phillipse, "Physics and applications of organic microcavity light emitting diodes," *J. Appl. Phys.* **80**, 6954-6964 (1996).
12. M. J. Cox, *Visual ergonomics*, (University of Bradford 1999).
13. G. W. Ford and W. H. Weber, "Electromagnetic interactions of molecules with metal surfaces," *Phys. Rep.* **113**, 195-287 (1984).
14. R. R. Chance, A. Prock and R. Silbey, "Molecular fluorescence and energy transfer near interfaces," *Adv. Chem. Phys.* **37**, 1-65 (1978).
15. E. A. Hinds, "Perturbative cavity quantum electrodynamics," in *Cavity Quantum Electrodynamics*, P. R. Berman, ed., (Academic, New York, 1994).
16. R. J. Glauber and M. L. Lewenstein, "Quantum optics of dielectric media," *Phys. Rev. A* **43**, 467-491 (1991).
17. Y. Xu, J. S. Vuckovic, R. K. Lee, O. J. Painter, A. Scherer, and A. Yariv, "Finite-difference time-domain calculation of spontaneous emission lifetime in a microcavity," *J. Opt. Soc. Am. B*, **16**, 465-474 (1999).

18. A. V. Tikhonravov, "Some theoretical aspects of thin-film optics and their applications," *Appl. Opt.* **32**, 5417-5426 (1993).
19. K. V. Popov, J. A. Dobrowolski, A. V. Tikhonravov and B. T. Sullivan, "Broadband high-reflection multilayer coatings at oblique angles of incidence," *Appl. Opt.* **36**, 2139-2151 (1997).
20. N. Matuschek, Franz X. Kartner and Ursula Keller, "Theory of double-chirped mirrors," *IEEE J. Sel. Top. Quantum Electron.* **4**, 197-208 (1998).
21. M. Gerken and D. A. B. Miller, "Wavelength demultiplexer using the spatial dispersion of multilayer thin-film structures," *Photonic Technol Lett.* **15**, 1097-1099 (2003).
22. B. T. Sullivan and J. A. Dobrowolski, "Implementation of a numerical needle method for thin-film design," *Appl. Opt.* **35**, 5484-5492 (1996).
23. A. V. Tikhonravov, M. K. Trubetskov and G. W. DeBell, "Application of the needle optimization technique to the design of optical coatings," *Appl. Opt.* **35**, 5493-5508 (1996).
24. J. A. Nelder and R. Mead, "A simplex method for function minimization," *Comput. J.* **7**, 308-313 (1965).
25. M. Deopura, C. K. Ullal, B. Temelkuran, and Y Fink, "Dielectric omnidirectional visible reflector," *Opt. Lett.* **26**, 1197-1199 (2001).
26. E. D. Palik, ed., *Handbook of optical constants of solids* (Academic, Boston 1999).
27. P. A. Lee, G. Said, R. Davis and T. H. Lim, "On the optical properties of some layer compounds," *J. Phys. Chem. Solids* **30**, 2719-2729 (1969).
28. M. A. Baldo, S. Lamansky, P. E. Burrows, M. E. Thompson and S. R. Forrest, "Very high-efficiency green organic light-emitting devices based on electrophosphorescence," *Appl. Phys. Lett.* **75**, 4-6 (1999).

Organic light-emitting devices (OLEDs) are efficient light sources with applications in displays and solid-state lighting [1-8]. Numerous research efforts over the last two decades have resulted in marked improvements in the luminous efficiency, lifetime, and color gamut of both small molecular weight and polymer OLEDs. However, a large fraction of the generated photons are wasted because they don't couple to useful free-space optical modes [1-6]. In a typical OLED, coupling of photons into waveguided (WG) modes, surface plasmon polariton (SPP) modes, and modes that are trapped in the substrate (ST) by total internal reflection at the substrate-air interface, result in only a small fraction of the emitted photons being coupled into unbound (UB) modes useful for lighting or display applications [1-6] (Fig. 1). The ratio of number of photons emitted into UB modes over the total number of photons emitted, is the outcoupling efficiency,  $\eta_{oc}$ . In small molecular weight OLEDs with randomly oriented emitting dipoles,  $\eta_{oc} \approx 20\%$ , while for polymer OLEDs, the emissive dipoles are usually assumed to be aligned in the substrate plane during the spin-coating process, resulting in  $\eta_{oc} \approx 30\%$  [6].

Various schemes to enhance the photon outcoupling efficiency have been explored and fall into two categories. The first approach is to modify the structure or geometry of the device such that a greater fraction of the optical modes of the structure are unbound and extend undiminished into free space. Examples of such approaches are substrate surface texturing [1-2], substrate microlenses [3-4], and scattering layers [5]. Since such schemes primarily address ST modes, they are appropriate for lighting and signage applications but might have limited use in displays due to pixel blurring. A second approach is to engineer the spatial profiles of the optical modes such that emission in the device active region couples efficiently only to UB modes. This approach also influences the spontaneous emission rate and the internal quantum efficiency through the Purcell effect [7-10]. Tailoring of the spatial profiles of optical modes for enhancing the external efficiency of LEDs has been experimentally demonstrated utilizing both one-dimensional (1D) [7-8] and two-dimensional (2D) [9-10] periodic structures. The use of 1D periodic structures known as distributed Bragg reflectors (DBRs) in OLEDs is limited since most organic emitters have broad spontaneous emission spectra of about  $\sim 75\text{nm}$  of full-width at half-maximum (FWHM) [1-8], leading to strong variations in brightness and color with angle [8]. Moreover, since the cavity formed by the DBR and metal cathode provides field enhancement at selective frequencies only and field suppression at others, such devices have almost no benefit in terms of overall power efficiency [11]. Two-dimensional periodic structuring suffers from similar shortcomings and requires high-resolution patterning [9-10].

In display applications, a Lambertian angular emission profile is desired to minimize eye strain and fatigue [12]. However, a Lambertian radiation pattern over the full forward half-

space uses a large fraction of the available optical energy for emission into angles nearly parallel to the substrate. We have developed a methodology to design 1D non-periodic dielectric multilayer stacks that, when inserted between the substrate and transparent anode of an OLED, provide improved  $\eta_{OC}$  while maintaining Lambertian emission within a specified viewing cone, even when the emission spectrum of organic molecules is very broad ( $\sim 75\text{nm}$  FWHM). This allows one to trade off viewing angle for brightness.

In an OLED, shown in Fig. 1, electrons and holes recombine in the emissive layer (EML) between the electron (ETL) and hole transport layer (HTL) leading to the formation of excitons. A fraction of the photons emitted by these excitons is extracted through the transparent electrode. The rate of spontaneous emission and the angular and spectral distribution of photon flux depend on the interaction of the exciton dipole transition moment with the optical modes supported by the device structure. The eigenmodes of a planar device structure can be represented by their frequency  $\omega$ , in-plane wave-vector  $k_{xy}$  (see Fig. 1) and polarization (s or p). The rate of spontaneous emission per unit area is [13-17]:

$$P = \sum_{r_{ex}} \sum_{p,s} \sum_{\omega} \sum_{k_{xy}} \frac{\omega}{2} \text{Im}(\mathbf{p}^* \cdot \mathbf{E}^l(r_{ex})) f(\mathbf{r}_{ex}) g(\omega), \quad (1)$$

where  $g(\omega)$  represents the normalized lineshape of exciton emission in free space,  $f(r_{ex})$  is the exciton density as a function of the distance,  $r_{ex}$ , from the metal cathode.  $\mathbf{p}$  is the electric transition dipole moment of the exciton, and  $\mathbf{E}^l$  is the self electric field of the dipole in eigenmode  $l$  specified by the polarization (s or p),  $\omega$ , and  $k_{xy}$ . One can show [13-14] that the electric field magnitude at the active cross-section in the emission layer can be written as:

$$\mathbf{E}^s = \left( \frac{k^2}{4\pi\epsilon_0\epsilon} \right) \frac{i}{2} \frac{k_{xy}}{k_z} \eta_1^s \mathbf{p}_{xy} \quad (2)$$

and

$$\mathbf{E}^p = \left( \frac{k^2}{4\pi\epsilon_0\epsilon} \right) \left( \frac{i}{2} \frac{k_{xy}k_z}{k^2} \eta_2^p \mathbf{p}_{xy} + \frac{i}{2} \frac{k_{xy}^3}{k^2k_z} \eta_1^p \mathbf{p}_z \right) \quad (3)$$

where  $\epsilon$  is dielectric constant of the emissive organic material,  $k^2 = \frac{\omega^2\epsilon}{c^2} = k_{xy}^2 + k_z^2$  (with

$\text{Im}\{k_z\} \geq 0$ ) and  $\eta_1^s$ ,  $\eta_1^p$  and  $\eta_2^p$  are related to the complex Fresnel reflection coefficients,  $R_n^l$ , calculated at the location of the excitons for a plane wave in eigenmode  $l$  incident on the top ( $n=1$ ) or bottom ( $n=2$ ) interface from the emissive layer as

$$\eta_{1(2)}^{s(p)} = \frac{(1 \pm R_1^{s(p)})(1 \pm R_2^{s(p)})}{1 - R_1^{s(p)}R_2^{s(p)}} \text{ with the + sign used for } \eta_1^{s(p)} \text{ and the - sign for } \eta_2^{s(p)}.$$

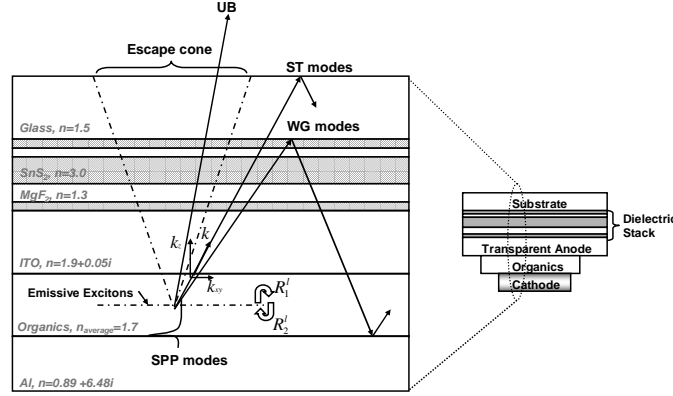


Fig. 1. OLED device structure with a non-periodic dielectric stack between the substrate and ITO anode. The various bound and unbound optical modes are identified: unbound modes (UB,  $k_{xy}c/\omega < 1$ ), substrate trapped modes (ST,  $1 < k_{xy}c/\omega < 1.5$ ), waveguided modes (WG,  $1.5 < k_{xy}c/\omega < 1.7$ ) and surface plasmon polariton modes (SPP,  $k_{xy}c/\omega > 1.7$ ).

The reflectivity of the bottom mirror,  $R_2^l$ , is largely determined by that of the metal cathode. The reflectivity of the top interface,  $R_1^l$ , can be modified by inserting a dielectric stack between the substrate and transparent anode. By simultaneously tailoring the amplitude and phase of  $R_1^l$  as a function of  $\omega$  and  $k_{xy}$ , such that  $|\mathbf{E}^l(r_{ex})|$  is minimal for ST, WG and SPP modes and maximal for UB modes,  $\eta_{OC}$  can be optimized.

It is possible to simultaneously design both the phase and amplitude of the reflectivity of a non-periodic dielectric multilayer stack [18]. Such non-periodic dielectric multilayers are widely used in passive devices like antireflection coatings, highly reflective polarization and angle-insensitive mirrors, spatially-dispersive wavelength division multiplexing mirrors, etc. [18-23]. We have developed a quasi-global optimization scheme for designing non-periodic dielectric stacks that optimize  $\eta_{OC}$  of an OLED within a specified viewing cone while maintaining a Lambertian emission profile for that viewing cone. Our scheme utilizes the needle optimization technique [22-23] for hopping between local optima in spaces of different dimensions coupled with the Nelder-Mead simplex method [24] for local optimization within the space of fixed dimension.

The optimization scheme starts with an OLED with a single layer in the dielectric stack. The performance the designs is measured by the root-mean-square deviation  $\delta$  between the fractional power emitted per unit solid angle  $P(\theta)$  and the desired target response  $f(\theta)$  within the viewing cone of half angle  $\theta_{view}$ :

$$\delta = \left[ \frac{1}{\theta_{view}} \int_0^{\theta_{view}} \left( \frac{P(\theta) - \beta_{OC} f(\theta)}{f(\theta)} \right)^2 d\theta \right]^{1/2} \quad (4)$$

where  $\theta$  is the azimuthal angle, and  $\beta_{OC}$  is the target apparent outcoupling efficiency.  $P(\theta)$  is evaluated using Eq. (1). The coefficients  $\eta_{1(2)}^{s(p)}(\omega, k_{xy})$  in Eqs. (2) and (3) are obtained using the transfer matrix approach. The characteristic matrices [22] for each layer are

stored as a function of  $\omega$  and  $k_{xy}$ . An exhaustive search is performed for the optimal location for insertion of a new layer and its optimal thickness. Since the characteristic matrices are stored, this exhaustive search only requires the calculation of three additional characteristic matrices for each tested structure. Repeated insertion of layers is performed before a Nelder-Mead simplex algorithm [24] is used for a local optimization of all layer thicknesses. Layers with a thicknesses  $<5\text{nm}$  are automatically removed from the design. This procedure is repeated until the desired performance is achieved or no further layers can be inserted without degrading performance.

Our stack designs are two component  $\text{SnS}_2/\text{MgF}_2$  coatings since it has been shown that optimal coatings are simple two-component coatings with the maximum and minimum available refractive indices [18].  $\text{SnS}_2$  and  $\text{MgF}_2$  have refractive indices of  $n=(3.0+0.002i)$  [25,26] and  $n=1.3$  [27] at  $\lambda=530\text{nm}$ , respectively. The OLED structure considered is glass/100nm indium-tin-oxide (ITO)/100nm organic layers/Al. Optical dispersion does not significantly change our results and was therefore ignored. Emitting dipoles are located at the center of the organic layer stack and their orientation is sampled from an isotropic distribution to model a small molecular weight OLED. The free space exciton emission spectrum is derived from an experimentally measured electroluminescence (EL) spectrum of the phosphorescent emitter  $\text{Ir}(\text{ppy})_3$  [28] by compensating for a wavelength-dependent Purcell factor calculated using Eq. (1). We further assume that the emitter has a quantum yield of unity. The control OLED structure achieves spectrally integrated coupling efficiencies into UB, ST, WG, and SPP modes of 23%, 21%, 10%, and 46% respectively. The EL spectrum (UB modes) peaks at  $\lambda=510\text{nm}$  and has a FWHM of 70nm.

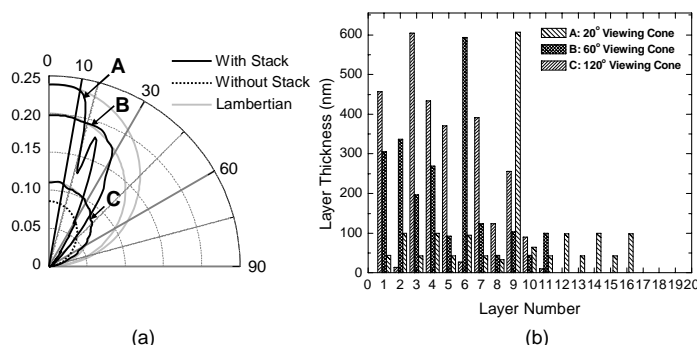


Fig. 2. (a). Spectrally integrated power emitted per unit solid angle vs. azimuthal angle for OLEDs with non-periodic dielectric stacks designs optimized for viewing cones of 20° (A), 60° (B) and 160° (C) (solid lines). The ideal Lambertian target responses (gray lines) and that of the control OLED (dotted line) are also shown (gray lines). (b) Thicknesses of the dielectric layers for the three designs shown in. All three structures have alternate layers of high ( $n=3.0$ ) and low ( $n=1.3$ ) index materials. The first layer is in contact with the substrate and is a high index layer in all three designs.

Figure 2(a) shows the calculated spectrally integrated angular response of OLEDs with three different non-periodic  $\text{SnS}_2/\text{MgF}_2$  stacks, A, B and C (solid lines), designed for optimal outcoupling into viewing cones of 20°, 60° and 160°, respectively. The spectrally integrated angular response of the control OLED (no stack, dotted line) and the ideal Lambertian response (gray lines) are plotted for comparison. The increase in brightness over the control OLED within the viewing cone is 232%, 179%, and 33% for designs A, B and C, respectively. The mean absolute deviation from the Lambertian within the targeted viewing cones is less than 1% for all designs. Figure 2(b) shows the thicknesses of the dielectric layers for designs A, B and C.

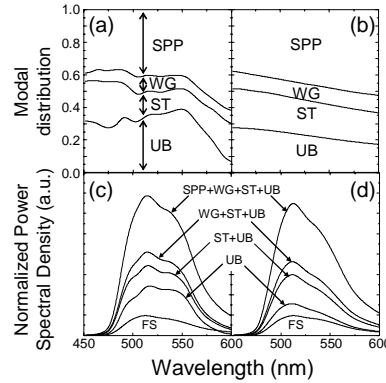


Fig. 3. (a). Fraction of emitted power into UB, ST, WG and SPP modes vs. wavelength for design C (120° viewing cone). (b) Same information as (a) for the control OLED. (c) Spectral power density of emitted radiation the various optical modes design C (120° viewing cone). The spectral power density distribution of the emitter in free space (FS, see text) is also shown. (d) Same information as (c) for the control OLED.

The non-periodic stacks increase the exciton coupling to selected UB modes (those that lie within the targeted viewing cone) and reduce the coupling for all other modes by redistributing the local photon density of states (LPDOS) [15-17]. This can be seen in Fig. 3(a), where the fraction of the optical power emitted into UB modes vs. wavelength is compared to that emitted in ST, WG and SPP modes for an OLED with stack design C (120° viewing cone). The same information for the control OLED is shown in Fig. 3(b). Most of the increase in  $\eta_{OC}$  is obtained by reducing the power emitted into ST modes. We also note that the power emitted into SPP modes is also substantially altered, indicating that stacks sandwiched between the substrate and transparent anode might be used to modify the coupling to SPP modes as well. As shown in Table 1, the total  $\eta_{OC}$  for design C is 33% compared to 23% for the control OLED. The apparent  $\eta_{OC}$ , i.e.  $\eta_{OC}$  that would be estimated based on observations within the viewing cone, is 35%.

The normalized spectral density into the various modes vs. wavelength is shown in Fig. 3(c) for design C and in Fig. 3(d) for the control OLED. The spectral power of the emitter in free-space is shown for reference (FS). The overall emission rate (SPP+WG+ST+UB) increases by 10% upon introduction of the non-periodic stack, showing that this approach does not substantially alter the overall radiative decay rate.

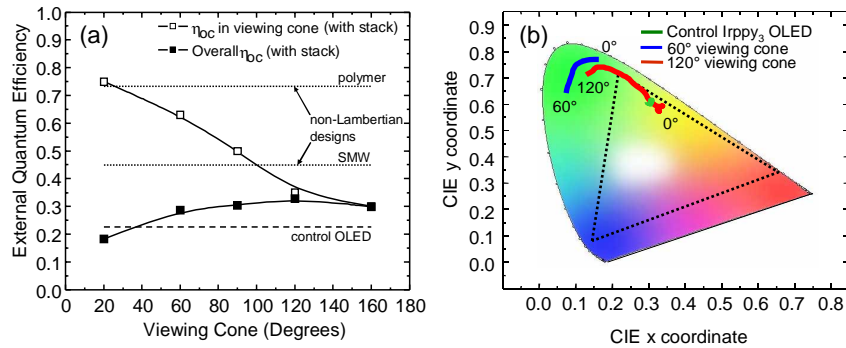


Fig. 4. (a). Relation between targeted viewing cone and total  $\eta_{OC}$  (filled squares) and apparent  $\eta_{OC}$  (open squares). The lines are a guide to the eye. For comparison purposes,  $\eta_{OC}$  for the control OLED is also shown (dashed line). For designs that are not subject to the Lambertian profile-constraint, total outcoupling efficiencies of 45% for a small molecular weight (SMW) and 73% for a polymer OLED can be obtained (dotted lines). (b) CIE vs. angle for the control OLED, and designs B (60° viewing cone) and C (120° viewing cone).

Table 1 summarizes the results obtained for designs targeting 20°, 60°, 90°, 120°, and 160° viewing cones. Figure 4(a) shows the achievable apparent  $\eta_{OC}$  within the viewing cone as a function of the viewing cone angular range targeted during stack optimization (open squares). The total  $\eta_{OC}$  (integrated for all angles) is also enhanced compared to a control OLED (dashed line) when optimized for designs with viewing angles  $>20^\circ$  (filled squares). In contrast, periodic photonic structures do not provide enhancement of the total  $\eta_{OC}$  for broadband emitters [11]. The apparent  $\eta_{OC}$  is 63% for design B (60° viewing cone). We note that if the constraint that the emission pattern is Lambertian is removed, total outcoupling efficiencies of 45% and 73% are obtained with optimized SnS<sub>2</sub>/MgF<sub>2</sub> stacks for small molecular weight and polymer OLEDs, respectively (dotted lines). The Commission Internationale de l'Eclairage (CIE) chromaticity coordinates vs. angle for the control OLED, designs B (60° viewing cone) and C (120° viewing cone) is shown in Fig. 4(b). The non-periodic stacks result in improved color saturation and an acceptable CIE chromaticity coordinate trajectory.

Table 1. Fraction of power emitted into the UB, ST, WG and SPP modes as a function of the angular range of the targeted viewing cone. The apparent  $\eta_{OC}$  within the viewing cone is also listed.

Viewing cone (°)	Fractional change in total radiative decay rate	Fractional change in radiative decay rate in UB modes	Power coupled into UB modes (%)	Power coupled into ST modes (%)	Power coupled into WG modes (%)	Power coupled into SPP modes (%)	Apparent Outcoupling Efficiency (%)
20	-0.06	-0.24	18	19	12	50	75
60	0.05	0.34	29	16	11	44	63
90	0.07	0.44	30	14	11	45	50
120	0.10	0.59	33	16	9	42	35
160	0.08	0.43	30	19	7	44	30

In conclusion, non-periodic dielectric stacks can be used to increase the outcoupling efficiencies of OLEDs while maintaining a Lambertian emission pattern. Tailoring of the stack design allows one to trade off brightness against viewing angle. A 2.7-fold increase in apparent  $\eta_{OC}$  and 26% increase in total  $\eta_{OC}$  is achievable for a 60° viewing cone compared to a control OLED. If a Lambertian response is not required, a 2-fold increase in total  $\eta_{OC}$  can be obtained for small molecular weight OLEDs. Because the dielectric stack lies outside the device structure region, it can be integrated with already optimized device structures without affecting electrical performance.

### Acknowledgments

The authors acknowledge support by the Semiconductor Research Corporation.